

Orientation of CRP-2A Core, Victoria Land Basin, Antarctica

T.S. PAULSEN^{1, 2}, T.J. WILSON², D. MOOS³, R.D. JARRARD⁴ & G.S. WILSON^{5, 6}

¹Department of Geology, University of Wisconsin-Oshkosh 800 Algoma Boulevard, Oshkosh, WI 54901 - USA

²Byrd Polar Research Center and Dept. of Geological Sciences, The Ohio State University, 1090 Carmack Road, Columbus, OH 43210 - USA

³Department of Geophysics, Stanford University Stanford, CA 94305-2215 - USA

⁴Department of Geology and Geophysics, University of Utah, 135 S. 1460 E., Rm. 719; Salt Lake City, UT 84112 - USA

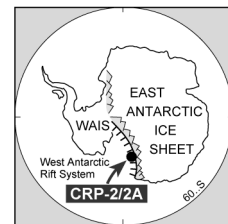
⁵Department of Earth Sciences, University of Oxford, Parks Road, Oxford, OX1 3PR - UK

⁶Institute of Geological and Nuclear Sciences, PO Box 30-368, Lower Hutt - New Zealand

*Corresponding author (paulsen@vaxa.cis.uwosh.edu)

Received 22 September 1999; accepted in revised form 30 May 2000

Abstract - Assessing the regional significance of structural and sedimentological features in core retrieved from the Cape Roberts Drilling Project (CRP-2A) requires the collection of orientated intervals of core. Orientated borehole televiwer (BHTV) data of the borehole walls was successfully collected from 199 to 450 metres below sea floor (mbsf). Within this interval, we utilised fracture mapping from the orientated BHTV record to reorientate core intervals by matching fractures in the borehole wall with correlative fractures in the core. Our results indicate that drilling-induced petal-centreline fractures have a strong preferred strike of $\sim N10^{\circ}W$ and that veins have a preferred strike of $\sim N30^{\circ}E$. We reorientated core outside the orientated BHTV interval by matching petal-centreline and core-edge fractures to the average orientation of petal-centreline and core-edge fractures found in the orientated BHTV interval. Our results from this method indicate that normal faults form a west-northwest-striking set and a poorly defined north-northeast set, and that veins form east-west and north-south-striking sets. A total of 244 metres ($\sim 39\%$) of the CRP-2A core has been reorientated by these fracture-matching methods to date. We also reorientated palaeomagnetic data using fracture matching between the core and the BHTV imagery to assess the palaeomagnetic method of core reorientation. Our results suggest that palaeomagnetic reorientation of the CRP-2A core is feasible if several criteria are satisfied: That at least 20 palaeomagnetic vectors are averaged within each intact core interval, that the palaeomagnetic vectors are distributed on one half of the stereonet (*i.e.* the vectors do not scatter around the center of the primitive circle), and that data is available to correct for bedding tilt in the intact core interval. We were unsuccessful at providing core orientation by matching the averages of the dip-direction of bedding in intact core, with the average dip-direction of bedding that was acquired from the dipmeter logs. However, future work may resolve problems with this technique and thus help provide orientation for other segments of the CRP-2A core.



INTRODUCTION

Direct orientation of core during drilling can be achieved by continuously scribing core within an orientated core barrel (Kulander et al., 1990). An alternative direct method was attempted in CRP-2A, using a downhole orientation tool designed to place orientated marks on the top of a core run prior to drilling. However the sole attempt to use the tool failed to provide direct orientation of the core run. In the absence of direct measurement, other means of determining core orientation were required in order to provide geographic coordinates for such directional core features as fracture planes, sedimentary depositional and deformational structures, and glacial structures. We therefore tried core reorientation methods that included: 1) matching fractures mapped in the borehole wall by the downhole borehole televiwer (BHTV) with correlative fractures in the core, 2) matching petal-centreline fractures in the core with the average orientation of petal-centreline fractures determined from the orientated BHTV imagery, 3) matching the average dip-direction of bedding measured

in intact core with the average dip-direction of bedding measured by the orientated downhole dipmeter tool, and 4) palaeomagnetic techniques. The purpose of this paper is to report the results of our efforts to reorientate the CRP-2A core.

Key initial steps in the reorientation process occurred during initial core logging at the drill site. These steps included identification of core runs that could be fitted together across run breaks, refitting core across fracture breaks, and logging of all fractures where spinning of the core between drilling and entry into the core barrel had disrupted the continuity of the core. Systematic examination and logging of all core breaks then allowed us to partition the core into intact intervals, which have undergone no internal rotations (Fig. 1). Each of these intact core intervals must be reorientated independently, since rotations between each may have occurred. In CRP-2A core, 364 independent core segments, ranging in length from 2 cm to 41 m, were logged. To date, our reorientation analysis has focused on the longer intact core segments.

Upon recovery and reconstruction of the core, red and

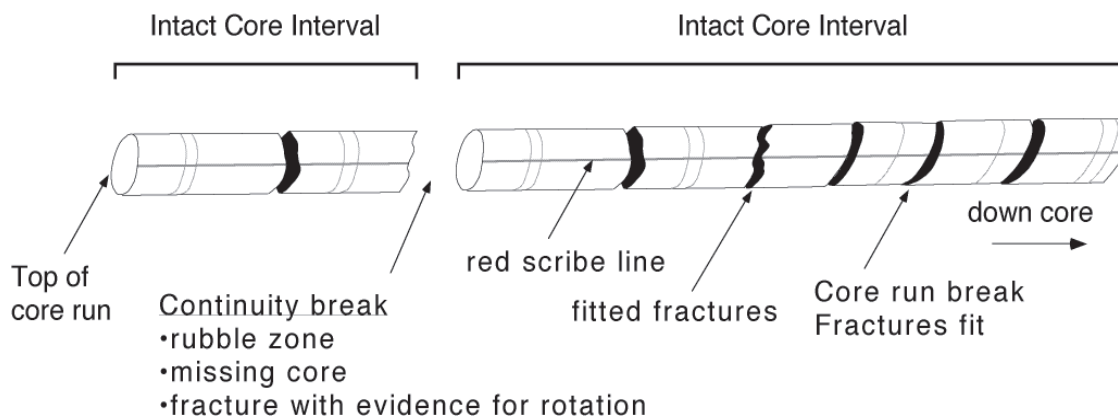


Fig. 1 - Sketch showing a typical intact core interval in which core segments could be fitted together along fracture planes within a core run or at run breaks (modified from Hailwood & Ding, 1995). The upper and lower boundaries of intact core intervals are where adjacent core could not be fitted together because of core loss, core rotation on fractures, and rubble zones. Fracture orientation was measured with respect to a red scribe drawn along the length of a core run.

blue scribe lines were drawn 180° apart along the length of the core. Dip and dip azimuth of all core fractures were measured with reference to the “arbitrary north” defined by the red scribe line (Fig. 1). Measured fractures were used to test the reliability of the core reorientation methods by conducting rotation cluster tests on drilling-induced and/or natural fractures found within the core (e.g. Hailwood & Ding, 1995). Fractures should show an improved clustering upon rotation back to in situ orientations because they typically form with systematic orientations with respect to a regional stress field (Lorenz et al., 1990; Kulander et al., 1990; Hailwood & Ding, 1995; Hamilton et al., 1995; Li & Schmitt, 1997). All core orientations reported in this paper use a magnetic declination correction of 148° based on the International Geomagnetic Reference Field (IGRF), which was confirmed by a field test near the drill site in August, 1999 (pers. comm. Alex Pyne). Tables 1 and 2 list the depth ranges for all core that was successfully reorientated to date. Those interested in using these results should contact T. Paulsen for details on the orientation procedure.

After the fracture measurements were made, the core was cut into one metre segments and fractures were studied and photographed further. In cases where the integrity of the core permitted handling, we then scanned the circumference of the surface of the core using Corescan®, equipment leased from DMT, Germany. The Corescan®, obtains digital images by rotating the whole core on rollers. We then joined the Corescan®, images of core segments within an intact core interval using DMT Corelog, software. Bedding dip directions and dip angles were determined with respect to the red scribe line by digitally outlining the trace of bedding using the ‘pick up structures’ command on the Corelog®, software. After we scanned the core, it was moved to the physical properties lab for analysis and then split lengthwise at $\sim 90^\circ$ to the scribe lines in half into two slabs, which were placed into an archive box and a working box.

BOREHOLE TELEVIEWER (BHTV)

Methodology: The Cape Roberts Science Team (1999) and Moos et al. (this volume) report on downhole borehole televiewer (BHTV) imagery collected to detect and delineate natural and induced fractures and stratigraphic features in the borehole walls, and to identify and characterize any stress-induced breakouts in the CRP-2A borehole. BHTV imagery was recorded from 65 to 164 mbsf and from 200 to 447 mbsf in the CRP 2A borehole. On-site problems with the BHTV magnetometer precluded recording the orientation of BHTV imagery of the upper portion of the borehole, but the orientation of imagery was successfully recorded in the lower portion of the borehole from 200 to 447 mbsf. Numerous subvertical fractures were recorded by the downhole BHTV tool at the same depths where steep, drilling-induced petal-centrelines or core-edge fractures were identified in the core (for discussion on fracture classification see Wilson and Paulsen, this volume, and references therein). Petal-centrelines fractures have curved shapes, becoming steeper in the downcore direction. Core-edge fractures in CRP-2A are subvertical, scoop-shaped ‘flakes’ that occur along the edge of the core. Petal-centrelines and core-edge fractures typically form with strike-lines that parallel SH_{max} and are typically modeled as tensile fractures following stress trajectories that radiate beneath the advancing drill bit. In cases where intact core intervals contained such drilling-induced fractures which could also be identified in the orientated BHTV imagery, it was possible to match the core fracture to the orientation of the borehole fracture and thereby orientate the core interval (e.g. Weber, 1994). Where possible, we matched dip-directions of core fractures and borehole fractures, yielding a unique orientation for the core. In some cases steep fractures occurred on one side of the core and borehole walls, which also allowed us to provide a unique core orientation. However, in many cases these relationships were ambiguous and our

Tab. 1 - Core orientated with BHTV.

Depth Range (mbsf)	Length (m)	Azimuth of RSL*
199.82-201.02	1.20	158°
201.59-207.02	5.43	055°
213.09-214.54	1.45	182°
214.65-224.92	10.27	026°
224.99-243.11	18.12	064°
243.11-246.35	3.24	334°
246.36-249.11	2.75	008°
250.29-256.26	5.97	307°
256.26-261.16	4.90	176°
261.16-267.16	6.00	228°
267.16-279.16	12.00	133°
293.58-302.62	9.04	018°
302.62-308.62	6.00	033°
308.62-309.59	0.97	156°
309.59-310.07	0.48	107°
310.07-317.63	7.57	088°
326.68-348.53	21.85	223°
354.01-359.54	5.53	251°
387.56-390.47	2.91	099°
436.03-437.56	1.53	319°
437.56-446.65	9.09	359°

*Azimuth of red scribe line at top of core interval

Tab. 2 - Core orientated with petal fractures.

Depth Range (mbsf)	Length (m)	Azimuth of RSL*
82.58 - 85.95	3.37	285°
132.71 - 135.34	2.63	203°
317.63 - 326.68	9.05	080°
455.69 - 467.67	11.98	240°
467.87 - 482.72	14.85	290°
518.96 - 527.74	8.78	006°
537.29 - 538.395	1.10	225°
540.14 - 543.88	3.74	090°
546.88 - 548.61	1.73	000°
554.24 - 556.86	2.62	210°
567.51 - 571.24	13.72	120°
577.23 - 618.07	40.84	192°

*Azimuth of red scribe line at top of core interval

there is potential to provide orientation where a series of fractures, such as conjugate fault systems, provide an unambiguous template.

MATCHING PETAL-CENTRELINE FRACTURES WITH BHTV-DETERMINED TREND

reorientation method relied on matching strike direction only. There is therefore a possible $\pm 180^\circ$ ambiguity in core orientation in many cases. This ambiguity does not affect interpretations that rely on strike-line trends, but unfortunately precludes the identification of conjugate fracture sets or regional bedding dip directions.

Results: BHTV-based reorientation of the CRP-2A core results in a better clustering of drilling-induced and natural fractures (Figs. 2, 3). After reorientation, petal-centreline and core-edge fractures form a well-defined N10°W striking set, whereas veins form a well-defined northeast-striking group. The tighter clustering of drilling-induced and natural fracture orientations after corrective rotation indicates that the BHTV-based reorientation method based on matching drilling-induced fractures was successful. The anomalous ~east-west orientations of some drilling-induced fractures may be due to their formation and propagation near pre-existing fractures (*cf.* Hamilton et al., 1995) or to an error in their classification as induced fractures. We have reorientated ~130 metres of core by this method (*i.e.*, ~21% of the CRP-2A core; Tab. 1). We estimate that if orientated BHTV imagery was collected from the entire borehole, we may have been able to double our orientation results just by matching steep, drilling-induced fractures in the core with correlatives in the borehole walls. Although our reorientation analysis has only focused on matching steep fractures in the core and borehole walls, possibilities exist for matching the dip-directions of other moderately dipping fractures, such as faults. In our preliminary analysis, we found ambiguities in correlating single, moderately-dipping fractures between the core and borehole because of local ambiguities in depth relationships between the core and borehole, and differences in the vertical extent of fractures due to the different diameters of the core and borehole. However,

Methodology: One method commonly used to reorientate drill core is to match natural fractures in unorientated core with the average orientation of fracture sets that occur in orientated core segments or in nearby rock outcrops (Kulander et al., 1990). One goal of the fracture studies of the Cape Roberts Drilling Project is to compare the orientation of faults within the CRP-2A core with the orientation of faults that cut bedrock outcrops onshore in the Transantarctic Mountains. Thus, we did not reorientate core by matching the orientation of faults within the core with the orientation of faults mapped onshore because this would preclude comparison of the onshore and offshore data sets. Instead, we matched the strike of individual, drilling-induced petal-centreline and core-edge fractures in unorientated intact core intervals with the average strike of petal-centreline and core-edge fractures (N10°W) determined from core that was reorientated using the BHTV imagery. This method assumes that the orientation of petal-centreline and core-edge fractures remains constant throughout the core. This assumption would hold if the *in situ* stress is uniform with depth, and there was no local perturbation of the stress field adjacent to pre-existing fractures or other anisotropies. As with the BHTV-based reorientation method, there is a $\pm 180^\circ$ ambiguity in core orientation because this method relies on matching the strike-lines of near-vertical fractures.

Results: Matching petal-centreline and core-edge fractures to the average orientation of petal-centreline and core-edge fractures in the orientated BHTV interval results in a better clustering of faults and veins (Figs. 4, 5). After reorientation, faults form a well-defined west-northwest striking set and veins form north-south and east-west striking groups. The tighter clustering of fracture orientations after corrective rotation indicates that matching

individual drilling-induced fractures with the calculated average induced-fracture strike can successfully reorientate intact core intervals. This implies that our assumption of constant orientation of induced fractures with depth is reasonable at CRP-2A. We were able to reorientate 114 metres of core by this method (*i.e.*, ~18% of the CRP-2A core). To date, our reorientation analysis has only focused on those sections of core that contain fractures veins and faults, but possibilities exist for using this method to reorientate other intact core intervals.

BEDDING DIP DIRECTIONS

Methodology: The Cape Roberts Science Team (1999) and Jarrard et al. (this volume) collected orientated downhole dipmeter data to identify and characterize the orientation of bedding and fractures within the CRP-2A borehole. Dipmeter data was collected from 63 - 160 mbsf and 200 - 623 mbsf in the CRP 2A borehole. In some segments of the CRP-2A core it was possible to obtain direct measurements of bedding and/or cross-bedding from whole-core Corescan® images. We tried to match bedding dip directions within the core with bedding dip directions measured by the downhole dipmeter tool (Jarrard et al., this volume).

The whole-core Corescan® analysis involved converting an image to grey scale, then picking all identifiable beds (excluding slumps, obvious soft-sediment

deformation, and drapes over limestones), and then labeling the bedding picks as either dubious or fair/good. Based on the bedding dips from an individual Corescan® file or a stitched Corescan® file of an intact core interval (the files varied 0.3 - 28.2 metres in length), we calculated an average bedding dip direction. This was a simple average azimuth, not a Fisher mean, excluding anomalous points, and including or excluding dubious bedding picks depending on azimuth and dip consistency within the core.

Dipmeter dip directions average at N75°E, corresponding to structural dip defined seismically (Henry et al., this volume). However, locally, dips are often dominated by depositional and postdepositional processes, plus the dip-direction tadpoles have substantial noise. Thus, we did not use the N75°E average, nor the dip-direction tadpoles from the depths corresponding to the intact core interval. Instead, we divided the dip data from the logged interval into zones of uniform bedding orientation that ranged from 5 - 60 m in length. We identified these zones based on the examination of dipmeter tadpole plots and of stereoplots of bedding perpendiculars. We split the longer zones into two, because of the abundance of data, so that we ended up with 27 intervals. We used Fisher statistics (Fisher et al., 1987) to determine mean dip azimuth, dip angle, and alpha-95 for each zone. We then matched the average bedding dip direction from each Corescan® file to the average dip azimuth determined for that depth interval from the dipmeter data. When a core was from an interval with no dipmeter data, adjacent

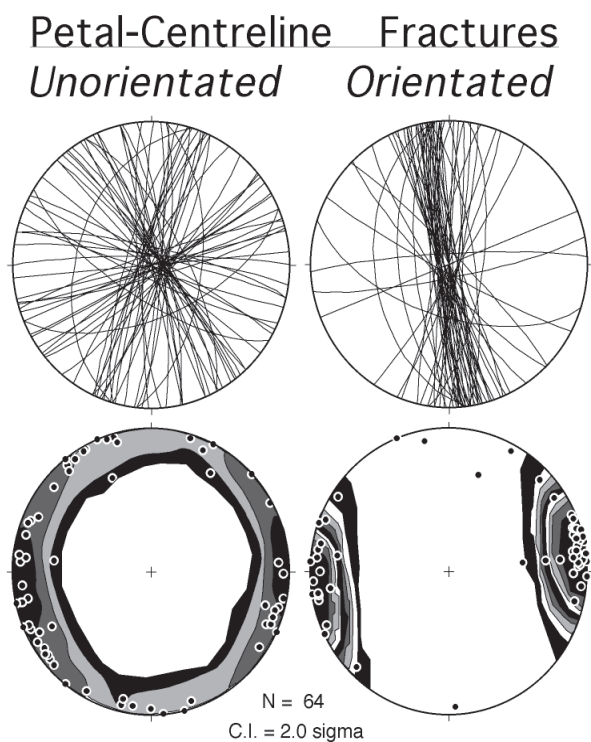


Fig. 2 - Equal area stereoplots (great circle and Kamb-contoured scatter plots) showing the orientations of petal-centreline fractures within core intervals that were reorientated utilizing fracture matching between BHTV imagery and core. Note the improved clustering after reorientation and that the reorientated petal-centreline fractures strike north-northwest. Data from 20 different intact core intervals, derived from depths ranging from ~200 to 400 mbsf.

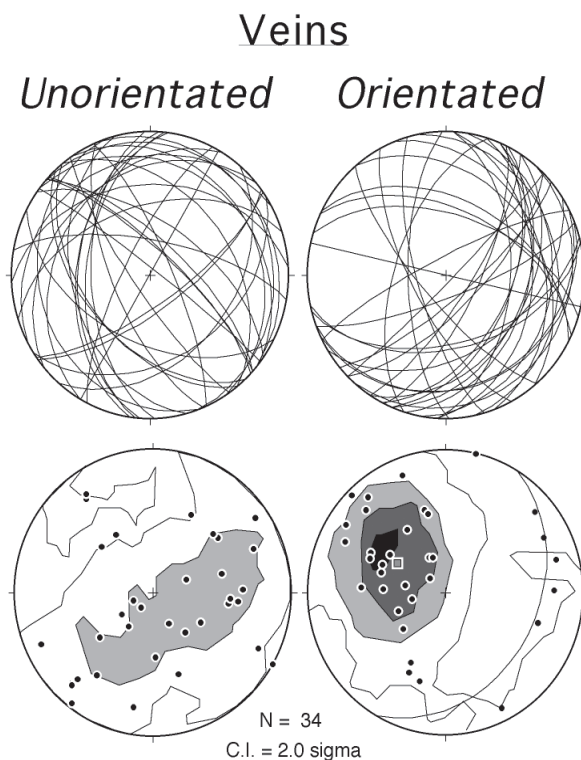


Fig. 3 - Equal area stereoplots (great circle and Kamb-contoured scatter plots) showing the orientations of veins within core intervals that were reorientated utilizing fracture matching between BHTV imagery and core. Note the improved clustering after reorientation and that the reorientated veins predominantly strike northeast. Data from 3 different intact core intervals, derived from depths ranging from 328 to 455 mbsf.

intervals typically began only a couple of metres away, so we used an average of mean azimuths from adjacent intervals.

Results: This core reorientation approach worked in general, but at this stage is probably associated with a high degree of error. For example, petal-centreline fractures show a better clustering after reorientation, but broadly fan around a north-south axis rather than displaying a tight cluster. Cluster tests of faults and veins also show ambiguous results. The overall failure of this approach may be due to several problems. In some cases the dipmeter interval average may not accurately reflect the orientation of bedding within a core segment, and thus result in an inaccurate reorientation of the core. We also observed an apparent clockwise drift of the red scribe line (arbitrary north) on the stitched Corescan® images. At this stage, we do not know if this drift of the scribe line has resulted in errors in determining the dip-direction of bedding in the Corescan® images. Further work should be able to evaluate the role of these potential problems and thus, whether bedding dip-direction can be used to reorientate additional intervals of the CRP-2A core.

PALAEOMAGNETISM

Methodology: In order to determine a magnetic polarity stratigraphy of the CRP-2A core, the Cape Roberts Science Team (1999) and Wilson et al. (this volume) drilled standard cylindrical palaeomagnetic samples every $ca. 0.5\text{m}$ from the working half of the core. All samples were collected perpendicular to the slab face of the split core and their angle of deviation with respect to the red scribe line recorded. This allowed us the possibility of utilising palaeomagnetic methods to reorientate continuous intervals of the core (*e.g.* Rolph et al., 1995; Paulsen and Wilson, 1998). The stable characteristic remanent magnetization (ChRM - the component of the magnetization that is dominant across the range of coercivity or thermal spectra for that sample) method was used in preference to the viscous remanent magnetization (VRM) method. This was because the VRM component of the natural remanent magnetization (NRM) of the core was typically overprinted by a drilling and/or core slabbing induced magnetization. ChRM directions were obtained by determining lines of best fit through demagnetization data and constrained by the origin on vector component plots (see Wilson et al., this volume). The ChRM method relies on the ability to determine an original detrital remanent magnetization (DRM), which is acquired at the time of deposition, as the magnetic particles align with the geomagnetic field.

Because DRM directions are acquired in a relatively short time period (less than *ca.* 2 k.y.), secular variation is not time averaged within individual palaeomagnetic samples. Therefore we focused our attention on the longest intervals of the CRP-2A core that could be reconstructed across run breaks and fractures and calculated average dipole directions within each intact core interval. We calculated mean palaeomagnetic vectors for 5 intact core intervals within the interval where orientated BHTV data

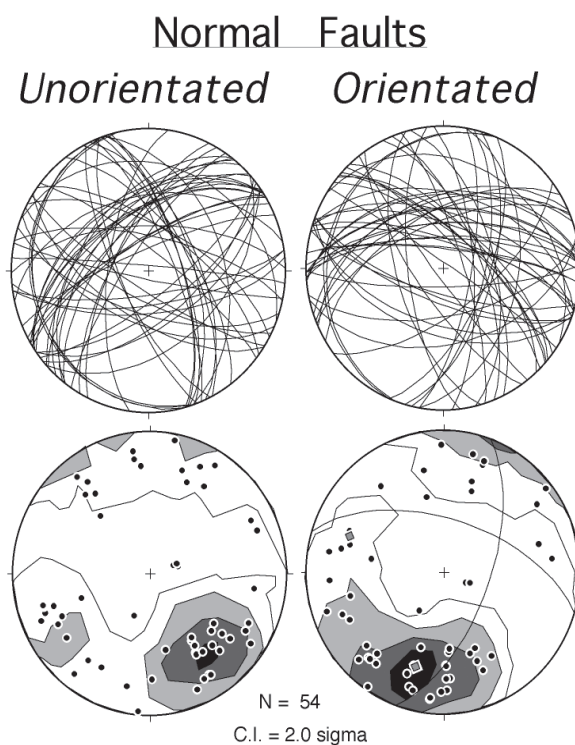


Fig. 4 - Equal area stereoplots (great circle and Kamb-contoured scatter plots) showing the orientations of normal faults within core intervals that were reorientated by matching petal-centreline and core-edge fractures with the average trend of petal-centreline and core-edge fractures that were reorientated by utilizing fracture matching between BHTV imagery and core. Note the improved clustering after reorientation and that the reorientated faults predominantly strike west-northwest and that a poorly defined second set strike north-northeast. Data from 9 different intact core intervals, derived from depths ranging from 132 to 618 mbsf.

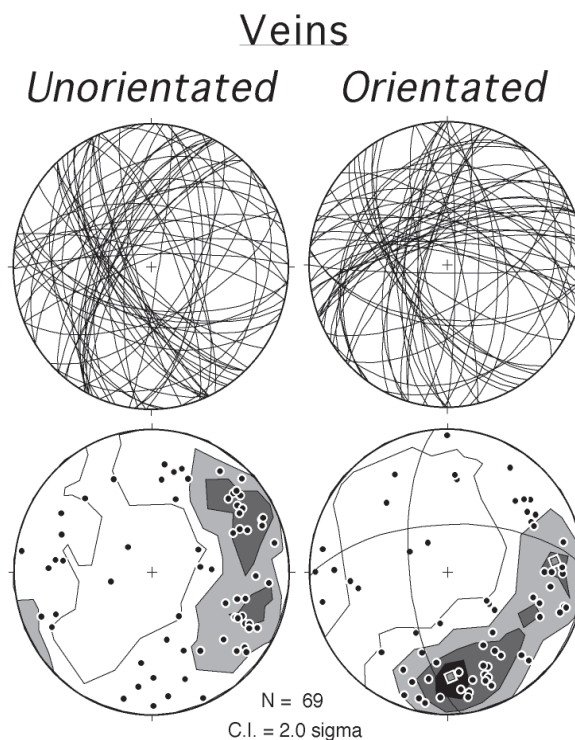


Fig. 5 - Equal area stereoplots (great circle and Kamb-contoured scatter plots) showing the orientations of veins within core intervals (Table 2) that were reorientated by matching petal-centreline and core-edge fractures with the average trend of petal-centreline and core-edge fractures that were reorientated by utilizing fracture matching between BHTV imagery and core. Note the improved clustering after reorientation and that the reorientated veins strike north-south and east-west.

was successfully collected (199 - 450 mbsf): 214.65 - 224.92 mbsf (22 samples), 224.99 - 243.11 mbsf (31 samples), 267.16 - 279.16 mbsf (15 samples), 326.68 - 348.53 mbsf (40 samples), and 437.56 - 446.65 mbsf (15 samples). Mean palaeomagnetic declination directions were calculated for each intact core interval using the procedure outlined in Paulsen and Wilson (1998), with two additional steps. 1) Each core interval and constituent palaeomagnetic vectors were rotated about a vertical axis to true north using the BHTV method, and 2) bedding and constituent palaeomagnetic vectors were rotated back to horizontal to return the vectors back to their depositional orientation. Jarrard et al. (this issue) conclude that the average dip-direction for 200-450 mbsf is about N87°E based on results from the downhole dipmeter tool. We therefore also rotated the data clockwise, looking south along a S3°E-trending axis, in order to account for the east dip of CRP2A strata (Cape Roberts Science Team, 1999). Seismic depth sections indicate that the dip angle of CRP2A strata increases with depth, probably due to growth faulting along a west-dipping normal fault located to the east of the drill site (see seismic section in Cape Roberts Science Team, 1999). To account for this increase in dip angle, we rotated core intervals 200 - 250 mbsf by 5.5°, 251 - 300 mbsf by 6.5°, and 301 - 450 mbsf by 7°, based on the seismic depth section of Henrys et al. (this volume). If the time averaged mean palaeomagnetic declination directions are reliable, the restoration steps outlined above should rotate the mean palaeomagnetic declination directions for normal polarity intervals to true north (000°N) and original mean palaeomagnetic declination directions for reversed polarity intervals to true south (180°S).

Results: Results for each intact core interval are presented in figure 6. Despite the high latitude of the CRP2A drill site, Fisher statistical parameters suggest that the calculated mean palaeomagnetic declination directions are reliable. In order to calculate the expected palaeomagnetic mean direction of the drill site, one has to take into account that the Antarctic continent has been in a stationary position with respect to the earth's hot spot reference frame during the time interval covered by the core intervals studied here (*i.e.*, the Oligocene; Barrett and Harwood, 1992). Thus, since the drill site is located at 78°S latitude, 12° latitude away from the expected time averaged magnetic pole (*i.e.*, the geographic south pole at 90°S), the palaeomagnetic mean direction is predicted to be 0° declination, -83° inclination. The mean palaeomagnetic inclinations calculated for each of the intact core intervals varies between -68° and -84°. Above the angular unconformity at 306.65 mbsf (Wilson et al., this volume, Henrys et al., this volume) mean palaeomagnetic inclination values are -75.9°, -84.4° and -83.1° for each of the three reorientated intact core intervals. These are within the statistical difference expected for such a high latitude. Below the angular unconformity at 306.65 mbsf, mean palaeomagnetic inclination values are -68.9° and -68.1° for each of the two reorientated intact core intervals considered in this study (Fig. 6). There are several plausible reasons for these shallow mean palaeomagnetic inclination values: First, it is possible that there is an inclination error in these lower/older strata.

Inclination errors can result in sediments where bioturbation is limited (Verosub, 1977) and where sediment has compacted significantly after deposition (Anson & Kodama, 1987 and Arason & Levi, 1990). Second, if there is a significant increase in easterly tectonic tilt below 306.65 m that we have not accounted for in the bedding corrections made above, this will have caused rotation and flattening of individual palaeomagnetic inclination values. Thirdly, the position of the Antarctic craton may have been displaced relative to the early Oligocene axial geocentric palaeomagnetic pole.

Mean palaeomagnetic declination values deviate from true north by only 13° to 15° if the mean palaeomagnetic declination directions can be calculated with >20 palaeomagnetic vectors that are distributed on one half of the stereonet (*i.e.* the vectors do not scatter around the center of the primitive circle, intervals 1 and 4 in Fig. 6). However, when mean declination directions are calculated by using a smaller number of vectors and/or vectors that scatter around the center of the primitive circle, then declination directions deviate from true north by up to 36° and the alpha-95 confidence ellipse intersects the vertical (Intervals 2 and 3, Fig. 6). This implies that the declination directions are less reliable for intervals 2 and 3. Interval 5 (438 - 447 mbsf, Fig. 6) provides an anomalous mean palaeomagnetic declination direction, suggesting that our BHTV-based estimate of core orientation may be incorrect. In summary, it should be possible to provide a rough estimate of orientation for other intervals of the CRP-2A core if >20 demagnetization vectors can be averaged over an intact core interval and be well clustered enough to lie on one half of the stereonet. The mean palaeomagnetic declination direction for all of the data from reorientated intervals 1 - 4 (the anomalous interval 5 is excluded) is close to true north (~14.7° declination, -77.1° inclination; Fig. 6). Not only is mean declination displaced slightly clockwise from that expected from a geocentric axial dipole field, but, also, the inclination of 77.1° is shallower than expected. However, the mean inclination value is biased by data from Interval 4 (326.68-348.53 mbsf; 37% of data) which lies below the inferred angular unconformity at 306.65 mbsf (Wilson et al., this volume). The deviation in mean declination may reflect a combination of up to five variables: subtle bias in the structural dip correction, local post-depositional sedimentary processes, movement between Antarctica and the axial dipole, subtle bias from the apparent clockwise drift of the red scribe line, and small block rotation (about a vertical axis) of the strata (and the mean palaeomagnetic declination directions) cored by CRP-2A (*cf.* Hamilton et al., 1998).

CONCLUSION

Initial results from a range of indirect core reorientation methods have reliably reorientated 39% of the CRP-2A drill core. Our results indicate that drilling-induced petal-centreline fractures have a strong preferred strike of ~N10°W and that veins have a preferred strike of ~N30°E. Since orientated BHTV imagery was not collected throughout the borehole, we reorientated core outside of

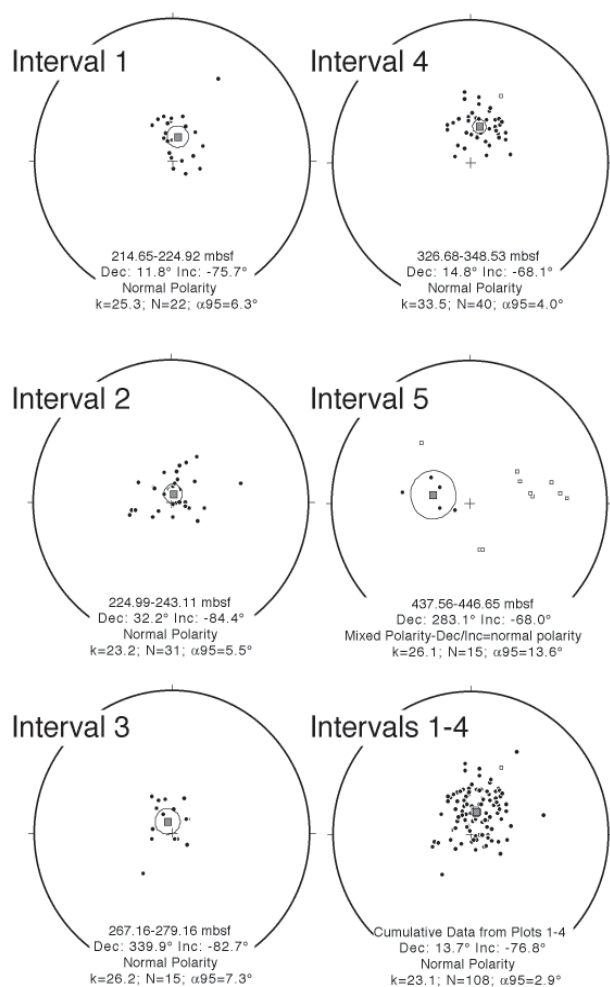


Fig. 6 - Equal area stereoplots showing individual palaeomagnetic declination vectors, calculated mean palaeomagnetic declination directions, and Fisher statistical parameters (Fisher et al., 1987) for each of the five intact core intervals. Filled dots represent palaeomagnetic demagnetisation vectors plotted in the upper hemisphere (normal polarity) and white squares represent palaeomagnetic demagnetisation vectors plotted in the lower hemisphere. Note that when the core is reorientated utilizing fracture matching between BHTV imagery and core, the mean palaeomagnetic declination directions are close to true north when based on >20 demagnetisation vectors that are well enough clustered so that they do not scatter around the center of the stereonet.

the orientated BHTV interval by rotating core so that petal-centrelines strike N10°W. Our results from this method indicate that normal faults form a west-northwest-striking set and a poorly defined north-northeast set, and that veins form east-west and north-south-striking sets. These reorientation methods result in a better clustering of fault and vein data, indicating that the reorientation methods have been successful, but in many cases do not provide a unique azimuthal orientation for the core because they rely on matching the strike-lines of steeply dipping fractures. We also assessed a palaeomagnetic method of orientating core by reorientating palaeomagnetic data using BHTV imagery. Our results suggest that palaeomagnetic reorientation of CRP-2A core may be feasible (within ~13 - 15° of true north), if the mean palaeomagnetic declination direction can be calculated with >20 palaeomagnetic vectors that are well clustered enough so that they do not scatter around a vertical axis.

Palaeomagnetic-based reorientation of the CRP-1 core did not use such well-clustered data (Paulsen and Wilson, 1998), and thus the reorientation estimates for CRP-1 core may be associated with a higher degree of error than has been previously estimated by Paulsen and Wilson (1998). Indeed, the average orientation of petal-centrelines fractures from the CRP-1 core is ~N10°E, nearly 20° from the mean orientation documented in this study. However, this analysis suggests that petal-centrelines fractures in the CRP-1 core could be rotated to the average orientation of petal-centrelines and core-edge fractures in the orientated BHTV interval of the CRP-2A core. If the *in situ* stress field is uniform at depth and between the CRP-1 and CRP-2A drill holes, then such rotations should refine the core reorientation estimates reported in Paulsen and Wilson (1998). This reorientation method could also serve to reorientate previously unorientated segments of CRP-1 core. We have also tried, but have been unsuccessful at, providing CRP-2A core orientation by matching the averages of the dip-direction of bedding in intact core, with the average dip-direction of bedding that was acquired from the dipmeter logs. Future work will concentrate on utilizing palaeomagnetic, bedding dip direction, and fracture matching techniques to provide orientation for other segments of the CRP-2A core.

ACKNOWLEDGEMENTS

This work was funded by NSF grant OPP-9527394 to T.J. Wilson, NSF grant OPP-9527319 to R. Jarrard, NSF grant OPP-9527412 to D. Moos, and FRST contract C05702 to Gary Wilson. Palaeomagnetic measurements were made by Gary Wilson, Fabio Florindo, Leonardo Sagnotti, and Andrew Roberts at the Cape Roberts Project palaeomagnetic laboratory in McMurdo Station (Cape Roberts Science Team, 1999); the downhole BHTV and dipmeter logging was conducted by Christian Bucker, Jason Brink, Erich Scholz and Thomas Wonik (Cape Roberts Science Team, 1999). Alex Pyne designed and deployed the core orientation tool. DMT provided access to the CoreScan and related core analysis software at reduced cost. We thank Rick Allmendinger and Neil Mancktelow for stereonet programs that greatly simplified our data analysis; and Bruce Luyendyk and Steve Schimmrich for reviews of the manuscript.

REFERENCES

- Anson G.L. & Kodama K.P., 1987. Compaction-induced shallowing of the post depositional remanent magnetisation in a synthetic sediment. *Geophysical Journal of the Royal Astronomical Society*, **88**, 7-23.
- Arason P. & Levi S., 1990. Compaction and inclination shallowing in deep sea sediments from the Pacific Ocean. *Journal of Geophysical Research*, **95**, 4501-4510.
- Barrett P.J. & Harwood D.M., 1992. Geological background and rationale for drilling. In Barrett P.J. & Davey F.J. (eds.), *Cape Roberts Project Workshop Report*. Royal Society of New Zealand, Miscellaneous Series, **23**, 4-10.
- Cape Roberts Science Team, 1999. Initial Report on CRP2/2A, Cape Roberts Project, Ross Sea, Antarctica. *Terra Antarctica*, **6**(1/2), 173p.

- Fisher N.I., Lewis T. & Embleton B.J.J., 1987. *Statistical Analysis of Spherical Data*. Cambridge, London, 329 p.
- Hailwood E.A. & Ding F., 1995. Palaeomagnetic reorientation of cores and the magnetic fabric of hydrocarbon reservoir sands. In: Turner P. & Turner A. (eds.), *Palaeomagnetic Applications in Hydrocarbon Exploration and Production*, Geological Society Special Publication No. 98, 245-258.
- Hamilton W.D., Van Alstine D.R., Butterworth J.E. & Raham G., 1995. Paleomagnetic orientation of fractures in Jean Marie Member cores from NE British Columbia/NW Alberta. *Petroleum Society of CIM, Annual Technical Meeting*, Banff, AB, May 14-17, 1995, Paper 95-56.
- Hamilton R.J., C.C. Sorlien C.C., Luyendyk B.P., Bartek L.R. & Henrys S.A., 1998. Tectonic regimes and structural trends off Cape Roberts, Antarctica. *Terra Antarctica*, **5**(3), 261-272.
- Kulander B.R., Dean S.L. & Ward B.J. Jr., 1990. *Fractured Core Analysis: Interpretation, Logging, and Use of Natural and Induced Fractures in Core*. American Association of Petroleum Geologists Methods in Exploration Series, No. 8, 88 p.
- Li Y. & Schmitt R., 1997. Well-bore bottom stress concentration and induced core fractures. *American Association of Petroleum Geologists Bulletin*, **81**, 1909-1925.
- Lorenz J.C., Finley S.J. & Warpinski N.R., 1990. Significance of coring-induced fractures in Mesaverde core, northwestern Colorado. *American Association of Petroleum Geologists Bulletin*, **74**, 1017-1029.
- Paulsen T. & Wilson G.S., 1998. Orientation of CRP-1 core. *Terra Antarctica*, **5**(3), 319-325.
- Rolph T.C., Shaw J., Harper T.R. & Hagan J.T., 1995. Viscous remanent magnetization: a tool for orientation of drill cores. In: Turner P. & Turner A. (eds.), *Palaeomagnetic Applications in Hydrocarbon Exploration and Production*, Geological Society Special Publication No. 98, 239-243.
- Verosub K.L., 1977. Depositional and postdepositional processes in the magnetisation of sediment. *Reviews of Geophysics and Space Physics*, **15**, 129-143.
- Weber H., 1994. Analyse geologischer Strukturen mit einem Bohrkernscanner [Analysis of geological structures using the DMT Corescan, machine]. *Felsbau*, **12**, no. 6, 401-403.